Journal of Magnetism and Magnetic Materials 364 (2014) 98–105

Contents lists available at ScienceDirect

Journal of Magnetism and Magnetic Materials

journal homepage: www.elsevier.com/locate/jmmm

# Rotating convection in a viscoelastic magnetic fluid

L.M. Pérez [a], D. Laroze [b,*], P. Díaz [c], J. Martinez-Mardones [d], H.L. Mancini [a]

[a] Departamento de Física y Matemática Aplicada, Universidad de Navarra, 31080 Pamplona, Spain
[b] Instituto de Alta Investigación, Universidad de Tarapacá, Casilla 7D, Arica, Chile
[c] Departamento de Ciencias Físicas, Universidad de La Frontera, Casilla 54 D, Temuco, Chile
[d] Instituto de Física, Pontificia Universidad Católica de Valparaíso, Casilla 4059, Valparaíso, Chile

ARTICLE INFO

*Article history:*
Received 3 January 2014
Received in revised form
5 April 2014
Available online 15 April 2014

*Keywords:*
Thermal convection
Magnetic fluid
Viscoelastic fluid

ABSTRACT

We report theoretical and numerical results on convection for a magnetic fluid in a viscoelastic carrier liquid under rotation. The viscoelastic properties are given by the Oldroyd model. We obtain explicit expressions for the convective thresholds in terms of the parameters of the system in the case of idealized boundary conditions. We also calculate numerically the convective thresholds for the case of realistic boundary conditions. The effects of the rheology and of the rotation rate on the instability thresholds for a diluted magnetic suspension are emphasized.



## 1. Introduction

Ferrofluids are stable colloidal suspensions of magnetic nanoparticles dispersed in a carrier liquid. In the absence of an external magnetic field the magnetic moments of the particles are randomly orientated and there is no net macroscopic magnetization. In an external field, however, the particles' magnetic moments easily orient and a large (induced) magnetization is present. There are two additional features in ferrofluids not found in ordinary fluids, the Kelvin force and the body couple [1]. In addition, in an external magnetic field, a ferrofluid exhibits additional rheological properties such as a field-dependent viscosity, special adhesion properties, and a non-Newtonian behavior [2]. Convection in ferrofluids has been a topic of great interest in the last decades. In addition, heat transfer through magnetic fluids has been of outstanding technological importance and was therefore also a leading area of scientific studies [3]. An important application of ferrofluids lies in the biomedical area where the carrier liquid is blood [4–8] which is known to have also special rheological properties [9–11]. In addition, when a magnetic field is applied, the ferrofluid can exhibit additional rheological properties such as magneto-viscosity, adhesion properties, and non-Newtonian behavior [12–22]. Hence, a detailed study of viscoelastic magnetic fluids is quite important and in order.

The first macroscopic description of magnetic fluids was given by Neuringer and Rosensweig [23]. The convective instability of a magnetic fluid layer heated from below in the presence of a uniform vertical magnetic field was discussed later by Finlayson [24]. Both cases, shear free and rigid horizontal boundaries were investigated within the linear stability method. Gotoh and Yamada [25] carried out a similar study by assuming the fluid to be confined between two magnetic pole pieces. A weakly nonlinear analysis in a strong external field was considered by Blennerhassett et al. [26]. The generalized Lorenz model for ferrofluid have been recently done by Laroze et al. [27]. The convective instability for a rotating layer in a magnetic fluid has been studied by Gupta and Gupta [28] and by Venkatasubramanian and Kaloni [29]. An amplitude equation for the stationary convection with idealized boundary condition was derived in Ref. [30]. The Küppers–Lortz instability for the case of a rotating magnetic fluid was formulated by Auernhammer and Brand [31]. Ryskin and Pleiner [32], using nonequilibrium thermodynamics, have derived a complete set of equations to describe ferrofluids in an external magnetic field. This description is made in terms of a binary mixture, where the magnetophoretic effect, as well as magnetic stresses, has been taken into account in the static and dynamic parts of the ferrofluid equations. When the magnetophoretic effect can be neglected, we have analyzed the thermal convection for rotating ferrofluids. For idealized boundary condition for the typical conductive state in the stationary case an analytical expression was found for the Rayleigh number as a function of control parameters [33]. Recently, the weakly nonlinear analysis for stationary convection in a rotating magnetic binary mixture was studied [34]. Other effects, such as the buoyancy-surface tension effects, nonuniform thermal gradients, and magnetization constitutive equations, have also been studied in Refs. [35–49].

A popular way to describe the viscoelastic properties of fluids is the use of a constitutive equation, which relates the stress and

* Corresponding author. Tel.: +56 582 230334; fax: +56 582 255371.
*E-mail address:* dlarozen@uta.cl (D. Laroze).

http://dx.doi.org/10.1016/j.jmmm.2014.04.027
0304-8853/

strain rate tensors. Rheology is the science devoted to generalize the linear, static Newtonian relation to the various, more complicated cases of non-Newtonian behavior. Very often an Oldroyd constitutive equation [50] is employed to realistically describe viscoelastic properties. In this model, the stress tensor is basically decomposed into both a polymeric-like elastic contribution and a Newtonian-like solvent contribution. Convection in such "Oldroyd fluids" has been studied by various authors for different physical and geometrical cases, e.g. both for free–free or rigid–rigid boundary condition [51–67]. By heating a fluid layer from below, as a general result, oscillatory modes can be obtained at onset in competition to the usual stationary convection states. Which type of instability, stationary or oscillatory, appears first, depends on the values of the rheological parameters. Experimental measurements of oscillatory convection in viscoelastic mixtures were reported by Kolodner [68] in a DNA suspension; and theoretical studies of the convection thresholds for binary viscoelastic mixtures in different types of fluids, can be found in Refs. [69–73]. Recently, studies on convection in viscoelastic magnetic fluid have been done [74–78].

The aim of this paper is to present the influence of the rotation and the viscoelasticity on convective cells in a magnetic fluid, in particular for cases, where the separation ratio and magnetic separation ratio are not too large and the simple fluid approximation can be used [32]. To this aim an Oldroyd viscoelastic magnetic fluid heated from below is considered. The description of the system involves many parameters whose values have not yet been determined accurately. Therefore, we are left with some freedom in fixing the parameter values. In order to be as exhaustive as possible, we will analyze the linear regime for two different limiting cases of boundary conditions i.e., the free–free (FF) and the rigid–rigid (RR) ones. In the first case (FF), one can analytically calculate the convection threshold as a function of the parameters of the fluid. In addition, we have further checked that we retrieve previous results obtained by other authors in simplified situations. In the case of realistic boundary conditions (RR), an analytical calculation is not tractable and we numerically solve the linearized system using a collocation spectral method, in order to determine the eigenfunctions and eigenvalues and consequently the convective thresholds. The paper is organized as follows: In Section 2, the basic hydrodynamic equations for viscoelastic magnetic fluid convection are presented. In Section 3 the linear stability analysis of the conduction state is performed. Finally, conclusions are presented in Section 4.

## 2. Basic equations

We consider a layer of incompressible magnetic fluid in a viscoelastic carrier liquid, of thickness $d$, parallel to the $xy$-plane, with very large horizontal extension, in a gravitational field $\mathbf{g}$ and subject to a vertical temperature gradient. The layer is rotating uniformly about the vertical axis with constant angular velocity $\boldsymbol{\varpi}$. The magnetic fluid properties can be modeled as electrically nonconducting superparamagnets. The magnetic field $\mathbf{H}$ is assumed to be oriented in a direction parallel to the $\hat{\mathbf{z}}$ axis. It would be homogeneous, if the magnetic fluid were absent. Let us choose the $z$-axis such that $\mathbf{g} = -g\hat{\mathbf{z}}$ and that the layer has its interfaces at coordinates $z = -d/2$ and $z = d/2$. A static temperature difference across the layer is imposed, $T(z=-d/2) = T_0 + \Delta T$ and $T(z=d/2) = T_0$. The set-up of the problem is drawn in Fig. 1. Under the Boussinesq approximation, the balance equations read

$$\nabla \cdot \mathbf{v} = 0, \tag{1}$$

$$\rho_0 d_t \mathbf{v} = -\nabla p + \nabla \cdot \overline{\boldsymbol{\tau}} + \rho \mathbf{g} + \mathbf{M} \cdot \nabla \mathbf{H} + 2\rho_0 \mathbf{v} \times \boldsymbol{\varpi}, \tag{2}$$

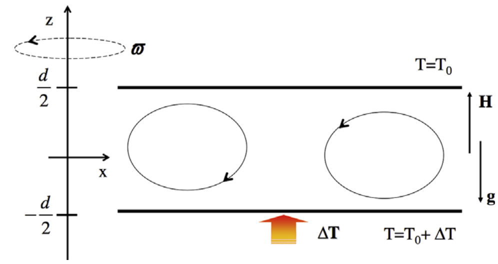


**Fig. 1.** A vertical cut through the fluid layer; the $y$-axis points into the $xz$-plane; the $z$-axis is the rotation axis.

$$\frac{c_{v,\mathbf{H}}}{T_0} d_t T + \chi_T \mathbf{H}_0 \cdot d_t \mathbf{H} = \overline{\kappa} \nabla^2 T, \tag{3}$$

where $d_t f = \partial_t f + \mathbf{v} \cdot \nabla f$ is the total derivative, $\mathbf{v} = \{v_x, v_y, v_z\}$ is the velocity field; $p$ is the effective pressure which contains the static hydrodynamic pressure, the gradient term of the magnetic force and the centrifugal contribution; $\rho$ is the mass density; $\rho_0$ is a reference mass density; $\overline{\boldsymbol{\tau}}$ is the extra stress tensor; $\mathbf{M}$ is the magnetization field; $c_{v,\mathbf{H}}$ is the specific heat capacity at constant volume and magnetic field, $T$ is the temperature, $T_0$ is a reference temperature; $\chi_T$ is the pyromagnetic coefficient and $\overline{\kappa}$ is the thermal diffusivity.

For the total density we use the following linear state equation [32]:

$$\rho = \rho_0 (1 - \alpha_T \Delta T + \alpha_H \mathbf{H}_0 \cdot \Delta \mathbf{H}) \tag{4}$$

where $\alpha_T$ and $\alpha_H$ are the thermal and the magnetic expansion coefficients, respectively. In the following, we denote $\Delta f = f - f_0$. In addition, for the magnetic field $\mathbf{H}$ and the magnetic induction $\mathbf{B}$, we suppose that the system is not conductive, i.e., it is governed by the static Maxwell equations

$$\nabla \times \mathbf{H} = \mathbf{0}, \tag{5}$$

$$\nabla \cdot \mathbf{B} = 0. \tag{6}$$

Furthermore, we assume a linear relationship between these fields, $\mathbf{B} = \mathbf{H} + \mathbf{M}$, and introduce the scalar magnetic potential $\mathbf{H} = -\nabla \phi$ to fulfill Eq. (5). The magnetization field is assumed to follow instantaneously the external field $\mathbf{M} = M(T, H)\hat{\mathbf{H}}$ with the usual phenomenological equation of state [24]

$$M(T, H) = M_0 - \chi_T \Delta T + \chi_H \mathbf{H}_0 \cdot \Delta \mathbf{H}. \tag{7}$$

A constitutive equation relating the extra stress tensor $\overline{\boldsymbol{\tau}}$ and the shear rate has also to be introduced. In a Newtonian incompressible fluid, the extra stress tensor is related to the strain tensor via the Newton law, $\overline{\boldsymbol{\tau}} = 2\nu \overline{\boldsymbol{D}}$, where $\overline{\boldsymbol{D}}$ is the symmetric part of the velocity field gradient and $\nu$ is the kinematic viscosity. For complex polymeric fluids, a more general constitutive relation between stress and strain rate $\overline{\boldsymbol{\tau}} = \overline{\boldsymbol{\tau}}(\overline{\boldsymbol{D}})$ is necessary to describe the behavior. This last relation is subject to symmetry restrictions. One type of constitutive relation that satisfies these symmetry requirements and that can be further justified by the kinetic theory of dumbbells has been proposed by Oldroyd [50]. This family of models, developed in the fifties of the last century, includes particular cases that are widely used for different kinds of polymeric solutions. In the general Oldroyd model, the constitutive equation is

$$(1 + \lambda_1 D_t) \overline{\boldsymbol{\tau}} = 2\nu (1 + \lambda_2 D_t) \overline{\mathbf{D}}, \tag{8}$$

where $\nu$ is the static viscosity, $\lambda_1$ is the relaxation time, and $\lambda_2$ is the retardation time; and the last two parameters characterize the viscoelastic time scales. For thermodynamic stability reasons both, $\lambda_1$ and $\lambda_2$ are taken to be positive. The symbol $D_t$ in Eq. (8) denotes a rotational invariant ("frame-indifferent") time derivative, defined as

$$D_t\overline{\boldsymbol{\tau}} = d_t\overline{\boldsymbol{\tau}} + \overline{\boldsymbol{\tau}}\cdot\overline{\mathbf{W}} - \overline{\mathbf{W}}\cdot\overline{\boldsymbol{\tau}} + a(\overline{\boldsymbol{\tau}}\cdot\overline{\mathbf{D}} + \overline{\mathbf{D}}\cdot\overline{\boldsymbol{\tau}}), \tag{9}$$

where $\overline{\mathbf{W}}$ is the skew-symmetric part of the velocity field gradient and $a$ is a phenomenological parameter between $-1$ and $+1$. For $a=-1$, one gets the lower convected Jeffrey's model (Oldroyd B), for $a=0$ one gets the so-called co-rotational Jeffrey's model, and $a=1$ describes the upper convected Jeffrey's model (Oldroyd A). Let us comment that the coefficient $a$ is not completely independent of the other rheological parameters [83]. Some limiting cases are $\lambda_2=0$ that leads to a Maxwellian fluid, while a Newtonian fluid requires both, $\lambda_1=0$ and $\lambda_2=0$.

Let us now analyze the boundary conditions (BCs) of the system. A static temperature difference across the layer is imposed, $T(z=-d/2)=T_0+\Delta T$ and $T(z=d/2)=T_0$; as the magnetic BCs we use the typical continuity conditions of the Maxwell equations, i.e., $\mathbf{n}\times(\mathbf{H}_{in}-\mathbf{H}_{ex})=\mathbf{0}$ and $\mathbf{n}\cdot(\mathbf{B}_{in}-\mathbf{B}_{ex})=0$, where $\mathbf{n}$ is a unit vector normal to the boundaries. For the velocity field we analyze two types of BCs, which will be introduced later in the text. Hence, from Eqs. (1) to (8) and using these boundary conditions the conductive, convection-free state is given by

$$\mathbf{v}_{con}=\mathbf{0}, \tag{10}$$

$$T_{con}(z)=\overline{T}-\beta z, \tag{11}$$

$$\mathbf{H}_{con}(z)=\mathbf{H}_0(1+\lambda\beta z), \tag{12}$$

where $\beta=(\Delta T/d)$ and $\lambda=\chi_T/(1+\chi_H)$. After some algebra, the equations for the dimensionless perturbations can be written as

$$\nabla\cdot\mathbf{v}=\mathbf{0} \tag{13}$$

$$P^{-1}d_t\mathbf{v}=-\nabla p+\nabla\cdot\overline{\boldsymbol{\tau}}+Ra\boldsymbol{\Sigma}+\sqrt{T_a}\mathbf{v}\times\hat{\mathbf{z}} \tag{14}$$

$$(1+\Gamma D_t)\overline{\boldsymbol{\tau}}=(1+\Gamma\Lambda D_t)\overline{\mathbf{D}} \tag{15}$$

$$d_t(\theta-M_4\partial_z\phi)=(1-M_4)v_z+\nabla^2\theta \tag{16}$$

$$(\partial_{zz}+M_3\nabla_\perp^2)\phi-\partial_z\theta=0 \tag{17}$$

$$\nabla^2\phi_{ext}=0 \tag{18}$$

where $\{\mathbf{v},\overline{\boldsymbol{\tau}},\theta,\phi\}$ are the dimensionless perturbations of the velocity, the extra stress tensor, the temperature, and the magnetic potential, respectively. We have used the abbreviations $\boldsymbol{\Sigma}=\Pi_1(\theta,\phi)\hat{\mathbf{z}}+M_1\theta\nabla(\partial_z\phi)$ with $\Pi_1=(1+M_1)\theta-(M_1-M_5)\partial_z\phi$ and $\nabla_\perp^2=\partial_{xx}+\partial_{yy}$. In Eqs. (13)–(18) the following groups of dimensionless numbers have been introduced: (a) (pure fluids) The Rayleigh number, $Ra=\alpha_T g\Delta T d^3/\kappa\nu$, accounting for buoyancy effects; and the Prandtl number, $P=\nu/\kappa$, relating viscous and thermal diffusion time scales. (b) (rotation in pure fluids) The Taylor number $T_a=(2\varpi d^2/\nu)^2$. (c) (magnetic fluids) The strength of the magnetic force relative to buoyancy is measured by the parameter $M_1=\beta\chi_T^2H_0^2/(\rho_0 g\alpha_T(1+\chi))$; the nonlinearity of the magnetization, $M_3=(1+\chi)/(1+\chi+\chi_H H_0^2)$, a measure of the deviation of the magnetization curve from the linear behavior $M_0=\chi H_0$; the relative strength of the temperature dependence of the magnetic susceptibility $M_4=\chi_T^2H_0^2T_0/c_H(1+\chi)$; and the ratio of magnetic variation of density with respect to thermal buoyancy $M_5=\alpha_H\chi_T H_0^2/(\alpha_T(1+\chi))$. (d) (viscoelastic fluids) The Deborah number, $\Gamma=\lambda_1\overline{\kappa}/d^2$, describing stress relaxation; and the ratio between retardation and stress relaxation times, $\Lambda=\lambda_2/\lambda_1$. Since $\lambda_{1,2}$ are positive, so are $\Gamma$ and $\Lambda$. For $\Gamma=0$ one recovers the Newtonian fluid, while for $\Lambda=0$ the Maxwellian fluid is obtained.

Let us comment on the numerical values of the parameters: $Ra$ and $T_a$ can be changed by several orders of magnitude, while a typical value for $P$ in viscoelastic fluids is $P\sim10^0-10^3$. The magnetic numbers have the following order of magnitude: $M_1\sim10^{-4}-10$, $M_3\gtrsim1$, $M_4\sim M_5\sim10^{-6}$ for typical magnetic field strengths [32,33]. For aqueous suspensions it is suggested that the Deborah number is about $\Gamma\sim10^{-3}$–$10^{-1}$ [68,79–81], but for other viscoelastic fluids the Deborah number can be of the order of $\Gamma\sim10^3$. Unfortunately, no experimental data are available for the retardation time , so we treat $\Lambda$ as arbitrary in the range $[0,1]$. In addition, the above set of equations is still unnecessarily complicated. We will simplify it first by neglecting $M_4$, which is a common simplification in the description of instabilities in ferrofluids [5]. Since $M_4$ is not related to viscoelastic effects, which we are interested in here, we expect not to loose any reasonable aspect of the problem under consideration. The same is true for the coefficient $M_5$. So, we take $M_4=0=M_5$ in the following analysis. Thus, we are left with two magnetic field-dependent effects characterized by the parameters $\{M_1,M_3\}$. The first one denotes the influence of the Kelvin force and is expected to have a dominant influence on the convection behavior. The second parameter, $M_3$ is different from 1 due to the intrinsic nonlinearity of the magnetization and is only a weak function of the external magnetic field. In the next sections we will develop the linear analysis for both stationary and oscillatory convection.

## 3. Linear stability analysis

In order to calculate the linear stability, we only need the linear parts of Eqs. (13)–(17). This is readily done by neglecting the advective terms $\mathbf{v}\cdot\nabla$ and replacing $D_t$ by $\partial_t$. Moreover, the effective pressure and two components of the velocity field can also be eliminated by applying the curl $(\nabla\times\cdots)$ and double curl $(\nabla\times\nabla\times\cdots)$ to the Navier–Stokes equation and then considering the z-components of the resulting equations, that is $v_z$ and $\zeta=(\nabla\times\mathbf{v})_z$ (i.e., the vertical components of the velocity and the vorticity). After some algebra, the linear equations read

$$P^{-1}\partial_t\Pi_t\nabla^2 v_z=\Xi_t\nabla^4 v_z-\sqrt{T_a}\Pi_t\partial_z\zeta+Ra\Pi_t\nabla_\perp^2\mathcal{L}_\Sigma \tag{19}$$

$$P^{-1}\partial_t\Pi_t\zeta=\Xi_t\nabla^2\zeta+\sqrt{T_a}\Pi_t\partial_z v_z \tag{20}$$

$$\partial_t\theta=v_z+\nabla^2\theta \tag{21}$$

$$(\partial_{zz}+M_3\nabla_\perp^2)\phi-\partial_z\theta=0 \tag{22}$$

where $\mathcal{L}_\Sigma=(1+M_1)\theta-M_1\partial_z\phi$, $\Pi_t=1+\Gamma\partial_t$ and $\Xi_t=1+\Gamma\Lambda\partial_t$. We remark that Eq. (20) is due to the rotation. In fact, when $T_a\to0$ the vorticity $\zeta$ is completely decoupled from the other variables. One can define the vector field $\mathbf{a}=(w,\zeta,\theta,\phi)^T$ that contains the variables relevant for the linear analysis. Using standard techniques [82], the spatial and temporal dependencies of $\mathbf{a}$ are separated using the normal mode expansion

$$\mathbf{a}(\mathbf{r},t)=\mathbf{A}(z)\exp[i\mathbf{k}\cdot\mathbf{r}_\perp+st], \tag{23}$$

with $\mathbf{A}=(W,Z,\Theta,\Phi)^T$, where $\mathbf{k}$ is the horizontal wavenumber vector of a perturbation, $\mathbf{r}_\perp$ is the horizontal vector position and $s=\sigma+i\Omega$ is the complex eigenvalue with $\sigma$ the growth factor of the perturbation and $\Omega$ its frequency. Using this ansatz, Eqs. (19)–(22) are reduced to the following coupled ordinary differential equations:

$$D^4W=\xi_1D^2W-\xi_2W+\xi_3DZ \\ +Ra(\xi_4\Theta-\xi_5D\Phi) \tag{24}$$

$$D^2Z=\xi_6Z-\xi_3DW \tag{25}$$

$$D^2\Theta=\xi_7\Theta-W \tag{26}$$

$$D^2\Phi=\xi_8\Phi+D\Theta \tag{27}$$

where $D^n f = \partial_z^n f$, $\xi_1 = 2k^2 + s\mathcal{Q}/P$, $\xi_2 = k^2(k^2 + s\mathcal{Q}/P)$, $\xi_3 = \sqrt{T_a}\mathcal{Q}$, $\xi_4 = k^2(1+M_1)\mathcal{Q}$, $\xi_5 = k^2 M_1 \mathcal{Q}$, $\xi_6 = k^2 + s\mathcal{Q}/P$, $\xi_7 = k^2 + s$ and $\xi_8 = M_3 k^2$, such that $\mathcal{Q} = (1+s\Gamma)/(1+s\Lambda\Gamma)$. In the following two subsections, we analyze the results of the linear stability analysis for the FF and RR boundary conditions.

### 3.1. Idealized boundary conditions (FF)

In order to solve the set of differential equations analytically, the following boundary conditions

$$D\Phi = \Theta = DZ = D^2 W = W = 0, \tag{28}$$

are imposed at $z = \pm 1/2$. The z-dependence of the eigenfunctions of the stability problem can then be described by simple sine and cosine functions. The eigenvalue problem produces a dispersion relation

$$\mathcal{P}(s) \equiv \sum_{i=0}^{5} a_i s^i = 0, \tag{29}$$

where $a_j$ are functions of the system parameters

$$a_5 = q^2 \Gamma^2 \varrho \tag{30}$$

$$a_4 = a_5(2 + q^2\Gamma(1+2P\Lambda)) \tag{31}$$

$$a_3 = 2q^2 a_5(1+P+P\Lambda) + P^2\pi^2 T_a \Gamma^2 \varrho + q^2\varrho(1 + q^4\Gamma^2 P\Lambda(2+P\Lambda)) - Ra\Gamma^2 k^2 P Q_{13} \tag{32}$$

$$\begin{aligned} a_2 = & -Ra\Gamma k^2 P Q_{13}(\Gamma\Lambda P q^2 + 2) \\ & + q^4 \varrho(\Gamma^2\Lambda^2 P^2 q^4 + 2P + 1) \\ & + 2\Gamma P q^6 \varrho(\Lambda + \Lambda P + 1) \\ & + \pi^2 \Gamma P^2 \varrho(\Gamma q^2 + 2) T_a \end{aligned} \tag{33}$$

$$\begin{aligned} a_1 = & -k^2 P Q_{13}(\Gamma(\Lambda+1)Pq^2 + 1)Ra \\ & + P q^6 \varrho(2\Gamma\Lambda P q^2 + P + 2) \\ & + \pi^2 P^2 \varrho(2\Gamma q^2 + 1) T_a \end{aligned} \tag{34}$$

$$a_0 = P^2 q^2(q^6\varrho - Ra k^2 Q_{13}) + \pi^2 P^2 q^2 \varrho T_a \tag{35}$$

where $q^2 = k^2 + \pi^2$ and $Q_{13} = k^2 M_1 M_3 + \varrho$ with $\varrho = M_3 k^2 + \pi^2$. Notice that $a_5$ and $a_4$ do not depend on $Ra$, while all other $a_j$ are of the form $a_j = a_j^I + a_j^{II} Ra$. In addition, Eq. (29) allows for an analytical expression of the Rayleigh number as a function of $\{s, k\}$

$$Ra = \frac{\varrho q^2(q^2+s)(Pq^2\gamma + s\epsilon)^2}{k^2 P\epsilon(s + Pq^2\gamma + s^2\Gamma)(k^2 M_1 M_3 + \varrho)} + \frac{\varrho(q^2+s)(\epsilon P\pi)^2 T_a}{k^2 P\epsilon(k^2 M_1 M_3 + \varrho)(s + Pq^2\gamma + s^2\Gamma)} \tag{36}$$

where $\gamma = 1 + s\Lambda\Gamma$ and $\epsilon = 1 + s\Gamma$. Let us analyze some particular cases. First, in the case without rotation, ($T_a$=0), the expression of Pérez et al. [77]

$$Ra \underset{T_a=0}{\longrightarrow} \frac{\varrho q^2(q^2+s)(Pq^2\gamma + s\epsilon)^2}{k^2 P\epsilon(s + Pq^2\gamma + s^2\Gamma)(k^2 M_1 M_3 + \varrho)} \tag{37}$$

is regained. Second, when the magnetic effects are neglected, ($M_1 = 0$ and $M_3 = 0$), Eq. (36) can be cast into the form

$$Ra \underset{M_1 = M_3 = 0}{\longrightarrow} \frac{(q^2+s)((P\pi\epsilon)^2 T_a + (Pq^3\gamma + sq\epsilon)^2)}{k^2 P\epsilon(s + Pq^2\gamma + s^2\Gamma)} \tag{38}$$

the result obtained by Laroze et al. [71]. Third, when the viscoelastic effects are neglected, ($\Gamma = 0$ ), Eq. (36) leads to

$$Ra \underset{\Gamma=0}{\longrightarrow} \frac{\varrho(q^2+s)(q^2(Pq^2+s)^2 + P^2\pi^2 T_a)}{k^2 P(Pq^2+s)(k^2 M_1 M_3 + \varrho)} \tag{39}$$

the case that was studied by Auernhammer and Brand et al. [31]. Finally, an important limit is $P \to \infty$, when the thermal diffusive time scale is much larger than the viscous one. This might be common for highly viscous fluids [82] and many viscoelastic liquids [50]. In that case one arrives at

$$Ra \underset{P\to\infty}{\longrightarrow} \frac{\varrho(q^2+s)(q^6\gamma^2 + \pi^2 T_a \epsilon^2)}{k^2 q^2 \gamma\epsilon(k^2 M_1 M_3 + \varrho)} \tag{40}$$

In general, there are two different bifurcation cases, a stationary one with $s$=0, and an oscillatory one that occurs when $s = i\Omega$ with $\Omega$ finite and real. For specific values of the parameters, the critical $Ra$ values of these two instabilities, $Ra_{sc}$ and $Ra_{oc}$, respectively, can be equal, thus constituting a codimension-2 bifurcation. We first consider the stationary case.

#### 3.1.1. Stationary bifurcation

In the stationary case ($s$=0), we find the marginal stability relation between the Rayleigh number and the wavenumber of the perturbation

$$Ra_s = \frac{(q^6 + \pi^2 T_a)\varrho}{k^2(k^2 M_3(1+M_1) + \pi^2)} \tag{41}$$

to be identical to that for a rotating ferrofluid [28,29]. Consequently, when the rotation is neglected, $Ra_s$ is reduced to

$$Ra_s \underset{T_a=0}{\longrightarrow} Ra_s^{[0]} = \frac{q^6\varrho}{k^2(k^2 M_3(1+M_1) + \pi^2)}, \tag{42}$$

which is the classical Finlayson result [24]. Note, that in the stationary case the viscoelastic effects do not appear at linear order. The minimum of the marginal curve (42) ($\partial_k Ra_s = 0$) gives the critical wavenumber $k_{sc}$ and, subsequently, the critical Rayleigh number, $Ra_{sc} = Ra_s(k_{sc})$, of the most unstable perturbation. Fig. 2 shows the rotation dependence of the linear threshold for different values of the magnetic field, where the field is represented by $M_1 \sim H^2$. We observe that $Ra_{sc}$ increases with increasing Taylor number, so the rotation rate has a stabilizing effect. In addition, $Ra_{sc}$ decreases for strong fields indicating the destabilizing effect of a magnetic field.

#### 3.1.2. Hopf bifurcation

We now discuss the oscillatory bifurcation. For a nonzero real frequency $\Omega$ the eigenvalue equation (36) is complex and constitutes two independent conditions. The real part gives the marginal stability curve $Ra_o(k, \Omega)$, while the imaginary part has to vanish, since $Ra$ is real. Using this condition we obtain an explicit equation for $\Omega$

$$\phi_0 + \phi_2\Omega^2 + \phi_4\Omega^4 + \phi_6\Omega^6 = 0 \tag{43}$$

where the coefficients $\{\phi_i\}$ are complicated functions of the parameters, explicitly given in the Appendix. After switching to

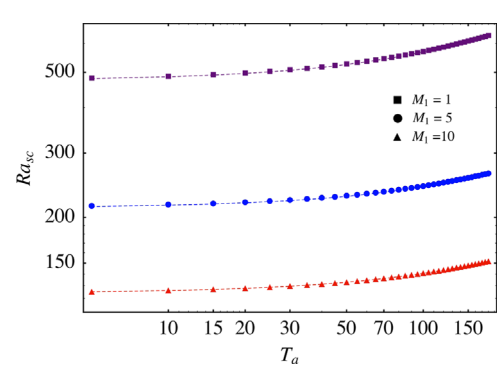


**Fig. 2.** The critical stationary Rayleigh number, $Ra_{sc}$, as a function of the Taylor number, $T_a$ for different values of $M_1$, at $M_3$=1.1.

the variable $\Phi=\Omega^2$, Eq. (43) can be reduced to

$$\phi_0+\phi_2\Phi+\phi_4\Phi^2+\phi_6\Phi^3=0, \tag{44}$$

which has the formal solution

$$\Phi_k=\frac{-1}{3\phi_6}\left(\phi_4+u_kC+\frac{\Delta_0}{Cu_k}\right), \tag{45}$$

where $k\in\{1,2,3\}$, $u_1=1$, $u_2=(-1+i\sqrt{3})/2$, $u_3=(-1-i\sqrt{3})/2$, and $C=\sqrt{[3]}(\Delta_1+\sqrt{\Delta_1^2-4\Delta_0^3})/2$ with $\Delta_0=\phi_4^2-3\phi_6\phi_2$ and $\Delta_1=2\phi_4^3-9\phi_6\phi_4\phi_2+27\phi_6^2\phi_0$. Since Eq. (45) describes different solution branches, the selection of the physical branch depends on the material parameters. Fig. 3 shows a three-dimensional plot of the frequency $\Omega$ as a function of both viscoelastic parameters $\Gamma$ and $\Lambda$. There are different branches with different values of $\Omega$. In the lower branch, for the parameters chosen the frequency decreases with increasing $\Lambda$, and close to the Newtonian case ($\Lambda=1$ and $\Gamma=0$) the instability must be stationary, hence the frequency is zero. Finally, let us remark that multiple solutions are typicality found in viscoelastic systems [65,66,73].

The oscillatory Rayleigh number, $Ra_o$, as a function of $\Omega$ and the control parameters is given by

$$\begin{aligned}\frac{Ra_o}{Ra_s}=&\frac{k^2(\pi^2P^2T_a-K\Omega^2)}{P(q^6+\pi^2T_a)}\\&+\frac{k^2K^2P(\Lambda(\Gamma K-1)+1)}{P\Gamma(q^6+\pi^2T_a)}\\&-\frac{k^2(\Lambda-1)K^2P(\Gamma K-1)}{P\Gamma(q^6+\pi^2T_a)(\Gamma^2\Omega^2+1)}\\&+\frac{\pi^2k^2KP^2T_a(K(1-P)-\Gamma\Omega^2\Pi_1)}{(q^6+\pi^2T_a)(\Gamma^2\Omega^4+K^2P^2+\Omega^2\Pi_2)}\end{aligned} \tag{46}$$

where $K=k^3+\pi^2$, $\Pi_1=\Lambda(\Gamma K(\Lambda P-1)+1)-1$, and $\Pi_2=\Gamma KP(\Lambda(\Gamma K\Lambda P+2)-2)+1$. Since the oscillatory Rayleigh number is proportional to the stationary Rayleigh number, a codimension-2 bifurcation can appear, if the right-hand side of Eq. (46) is equal to one. Since the latter does not depend on the magnetic contributions, the oscillatory instability is, at the linear level, a consequence of the rotation or the viscoelasticity, or a mixture of both effects.

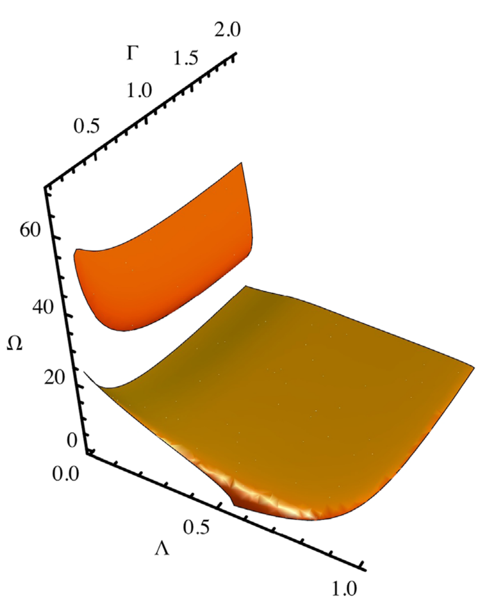


**Fig. 3.** The frequency $\Omega$ as a function of both viscoelastic parameters $\Lambda$ and $\Gamma$ at $k=4$, $P=10$ and $T_a=50$.

We now discuss some limiting cases. First, for $T_a=0$, the Rayleigh number is reduced to

$$\frac{Ra_o}{Ra_s^{[0]}}\xrightarrow[T_a=0]{}\Lambda+\frac{1-\Lambda}{q^4}\left(\frac{q^2}{\Gamma}-\frac{q^2}{\Gamma\Xi_{[0]}}+\frac{q^4}{\Xi_{[0]}}\right)-\frac{\Omega_{[0]}^2}{Pq^4} \tag{47}$$

with $\Xi_{[0]}=1+(\Gamma\Omega_{[0]})^2$ and $Ra_s^{[0]}$ given by Eq. (42). In this case the corresponding frequency, $\Omega_{[0]}$, can be given in closed form

$$\Omega_{[0]}^2=\frac{q^2P\Gamma(1-\Lambda)-(1+P)}{\Gamma^2(1+P\Lambda)}. \tag{48}$$

For real $\Omega_0$ its square has to be positive. Obviously, for $T_a=0$ this cannot be achieved at all for Newtonian fluids and poses a lower limit on the Deborah number for Oldroyd (and Maxwell) fluids, $\Gamma\geq(1+P)/(Pq^2(1-\Lambda))$, which also means $\Lambda$ must not reach the value 1. This result was previously derived by Pérez and co-workers in Ref. [77].

Another limit that allows for an analytical solution is $P\to\infty$, where we find

$$\begin{aligned}\frac{Ra_o}{Ra_s}\xrightarrow[P\to\infty]{}&\frac{1}{(1+\Gamma^2\Lambda^2\Omega_{[\infty]}^2)\Xi_{[\infty]}}\\&+\frac{q^4\Gamma(1-\Lambda+q^2\Gamma\Lambda(1+\Lambda))\Omega_{[\infty]}^2}{\Xi_{[\infty]}(q^6+\pi^2T_a)(1+\Gamma^2\Lambda^2\Omega_{[\infty]}^2)}\\&+\frac{q^4\Lambda^2\Gamma^3(1-\Lambda+q^2\Gamma\Lambda)\Omega_{[\infty]}^4}{\Xi_{[\infty]}(q^6+\pi^2T_a)(1+\Gamma^2\Lambda^2\Omega_{[\infty]}^2)}\\&+\frac{\pi^2T_a\Gamma(-1+\Lambda+q^2\Gamma(1+\Lambda))\Omega_{[\infty]}^2}{q^2\Xi_{[\infty]}(q^6+\pi^2T_a)(1+\Gamma^2\Lambda^2\Omega_{[\infty]}^2)}\\&+\frac{\pi^2T_a\Gamma^3(-1+\Lambda+q^2\Gamma\Lambda)\Omega_{[\infty]}^4}{q^2\Xi_{[\infty]}(q^6+\pi^2T_a)(1+\Gamma^2\Lambda^2\Omega_{[\infty]}^2)}\end{aligned} \tag{49}$$

with $\Xi_{[\infty]}=1+(\Gamma\Omega_{[\infty]})^2$, such that

$$\begin{aligned}\Omega_{[\infty]}^2=&\frac{q^6(q^2\Gamma(1-\Lambda)\Lambda-(1+\Lambda))}{2\Gamma^2(\pi^2T_a+q^6\Lambda^2)}\\&-\frac{\pi^2T_a(1+\Lambda+q^2\Gamma(1-\Lambda))}{2\Gamma^2\Lambda(\pi^2T_a+q^6\Lambda^2)}\\&+\frac{(1-\Lambda)\sqrt{\pi^4T_a^2(1+q^2\Gamma)^2+\Psi}}{2\Gamma^2\Lambda(\pi^2T_a+q^6\Lambda^2)},\end{aligned} \tag{50}$$

where
$\Psi=\Lambda^2q^{12}(\Gamma\Lambda q^2+1)^2-2\pi^2\Lambda q^6T_a(\Gamma q^2(-3\Lambda+\Gamma\Lambda q^2-3)+1)$.

To calculate the oscillatory thresholds one first determines the critical wave number $k_{oc}$ that leads to the lowest threshold ($\partial_kRa_o=0$) which then gives to the critical Rayleigh number $Ra_{oc}=Ra_o(k_{oc})$ and critical frequency $\Omega_c=\Omega(k_{oc})$. For the general case this has to be done numerically.

Fig. 4 shows the critical oscillatory Rayleigh number, $Ra_{oc}$, as a function of the retardation to relaxation time ratio, $\Lambda$, for different values of the Deborah number $\Gamma$. We observe that for small $\Lambda$ ($\Lambda<0.1$) the value of the critical oscillatory Rayleigh number increases when $\Lambda$ increases until it reaches a local maximum, followed by a slight decrease to a shallow minimum, before it starts to increase again for all higher values of $\Lambda$. The topology of this curve is the same for all three values of $\Gamma$ considered, and only the heights and the positions of the local maxima and minima are slightly different.

Fig. 5 shows the corresponding critical frequency, $\Omega_c$, as a function of $\Lambda$, for different values of Deborah number $\Gamma$. For small $\Lambda(\lesssim 0.06)$ the frequency increases with $\Lambda$. A linear decrease follows, approximately up to those $\Lambda$ values, where $Ra_{oc}$ shows the shallow minimum. Beyond that, for $\Lambda\gtrsim 0.15$, the critical frequency decays exponentially. Similar to the case of the critical Rayleigh number, the $\Omega_c(\Lambda)$ curves have similar shapes for all Deborah numbers,

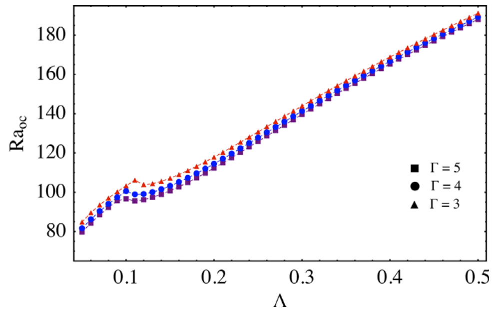


**Fig. 4.** $Ra_{oc}$ as a function of $\Lambda$ at $P=10$, $M_1=10$, $M_3=1.1$ and $T_a=10$ for different values of $\Gamma$, from bottom to top, $\Gamma=\{5,4,3\}=\{\blacksquare,\bullet,\blacktriangle\}$.

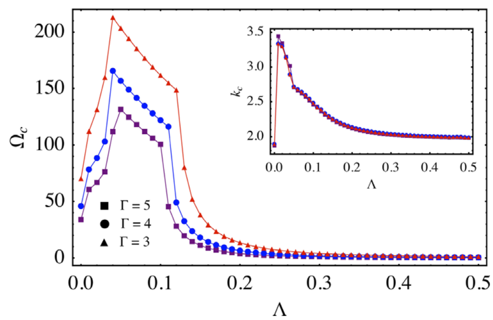


**Fig. 5.** $\Omega_c$ as a function $\Lambda$ for different values of $\Gamma$. The inset shows the critical wave number, $k_c$, as a function $\Lambda$ for different values of $\Gamma$. The fixed parameters are the same as in Fig. 4.

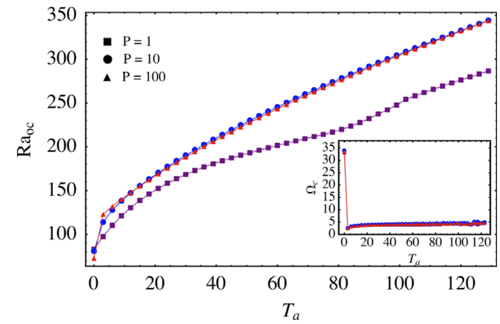


**Fig. 6.** $Ra_{oc}$ as a function of $T_a$ at $\Gamma=1$, $\Lambda=0.2$, $M_1=10$ and $M_3=1.1$ for different values of $P$, from bottom to top, $P=\{1,10,10^2\}=\{\blacksquare,\bullet,\blacktriangle\}$. The inset shows $\Omega_c$, correspondingly.

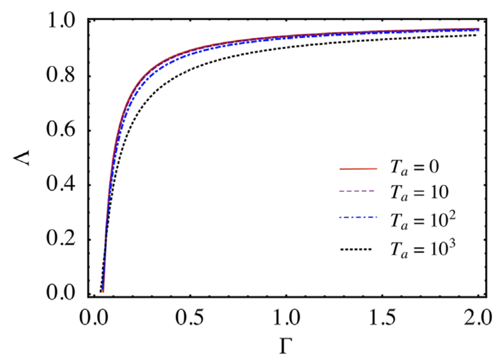


**Fig. 7.** The codimension-2 bifurcation line, $Ra_{sc}=Ra_{oc}$, that separates the stationary instability region (above) from the oscillatory one (below) at $M_1=10$, $M_3=1.1$, and in the limit $P\to\infty$, for different values of $T_a$, from top to bottom, $T_a=\{0,10,100,1000\}=\{$full, dashed, dash-dotted, dotted$\}$ line.

considered, although the actual numerical values are considerably different, at least for $\Lambda<0.3$. The inset of Fig. 5 shows the corresponding critical wavenumber, $k_c$. It is almost independent of $\Gamma$ and decreases by almost a factor of two before it reaches a plateau value for $\Lambda>0.3$.

Fig. 6 shows the critical oscillatory Rayleigh number, $Ra_{oc}$, as a function of the Taylor number, $T_a$, for different values of Prandtl number, $P$. The function $Ra_{oc}(T_a)$ is monotonically increasing denoting the stabilizing effect of the rotation. A similar behavior has been found in the stationary case. Increasing Prandtl numbers, on the other hand, reduces the threshold values, but does not change the global structure of $Ra_{oc}(T_a)$ and is rather small for the relevant values of $P\gtrsim 10$ [50]. The inset of Fig. 6 shows that the corresponding critical frequency, $\Omega_c$, is rather insensitive to both, the Prandtl number and the Taylor number.

### 3.1.3. Codimension-2 bifurcation

There exists a range of parameters where the critical oscillatory and stationary Rayleigh numbers have the same value, $Ra_{sc}=Ra_{oc}$. This is possible due to the non-Newtonian properties of the fluid layer. Fig. 7 shows this line separating the stationary instability regime (above) from the oscillatory one (below) in the $\Gamma-\Lambda$ space for different values of $T_a$. For $T_a\lesssim 100$ the influence of the rotation is rather weak, since $Ra_{oc}$ and $Ra_{sc}$ have a similar $T_a$ dependence. Nevertheless, for higher values of the rotation rate the oscillatory regime becomes smaller.

## 3.2. Realistic boundary conditions (RR)

The use of free–free boundary conditions at the two horizontal boundaries is a useful mathematical simplification, but does not reflect the physical reality, generally. The correct boundary conditions for viscous or viscoelastic fluids are

$$Z=W=DW=\Theta=0, \tag{51}$$

at the two horizontal rigid boundaries. In addition, in the case of a finite magnetic permeability $\chi_b$ of the rigid boundaries, the scalar magnetic potential must satisfy

$$(1+\chi_b)D\Phi\pm k\Phi=0, \tag{52}$$

at $z=\pm 1/2$, respectively [24]. Only in the limit $\chi_b\to\infty$, Eq. (52) tends to $D\Phi=0$.

In order to solve Eqs. (24)–(26) with these realistic boundary conditions, we use a spectral collocation method. Spectral methods ensure an exponential convergence to the solution and are the best available numerical techniques for solving simple eigenvalue – eigenfunction problems. Here, we follow the technique of collocation points on a Chebyschev grid as described by Trefethen [84]. The collocation points (Gauss-Lobatto) are located at height $z_j=\cos(j\pi/N)$ where the index $j$ runs from $j=N$ to $j=0$. Note that here the $z$-variable ranges from $-1$ to $+1$ and one has therefore to rescale Eqs. (24)–(26) accordingly, because the physical domain is defined in the range $(-1/2,+1/2)$. We use $N=40$ collocation points in the vertical direction, for which the equations and the boundary conditions are expressed. By using the collocation method, the set of differential equations (24)–(26) is transformed into a set of linear algebraic equations. The eigenfunctions $(\Theta(z),\Phi(z),W(z))$ are transformed into eigenvectors defined at the collocation points, $\mathbf{X}=(\Theta_N,\ldots,W_0)$, such that $\Psi_j=\Psi(z_j)$. After this stage of discretization, one is left with a classical generalized eigenvalue problem, $\overline{\mathbf{A}}\mathbf{X}=Ra\overline{\mathbf{B}}\mathbf{X}$, where $Ra$ and $\mathbf{X}$ are the eigenvalue and eigenvector, respectively.

In the case of the oscillatory instability considered here, one has to make sure that $Ra$ (as being a physical quantity) is a real number by choosing a correct value for $\Omega$. Therefore, one is left with a triplet $\{Ra,k,\Omega\}$ that defines a marginal stability condition (for a fixed value of the horizontal wavenumber $k$). This procedure is repeated for several values of $k$ leading to the marginal stability

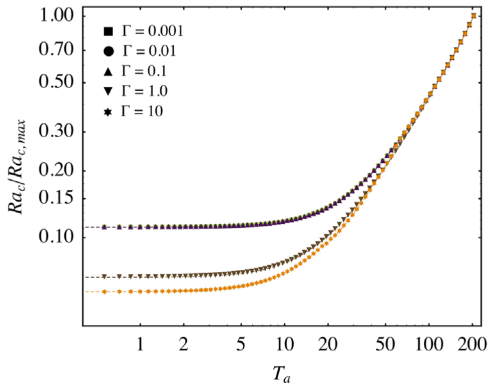


**Fig. 8.** (Color online) The normalized critical Rayleigh number $Ra_c/Ra_{c,\max}$ as a function of $T_a$ at $\Lambda = 0.5$, $P = 10$, $M_1 = 0.1$ and $M_3 = 1.1$ for different values of $\Gamma$, from bottom to top, $\Gamma = \{10^{-3}, 10^{-2}, 10^{-1}, 1, 10\} = \{■, ●, ▴, ▾, ✱\}$ for rigid–rigid boundary conditions.

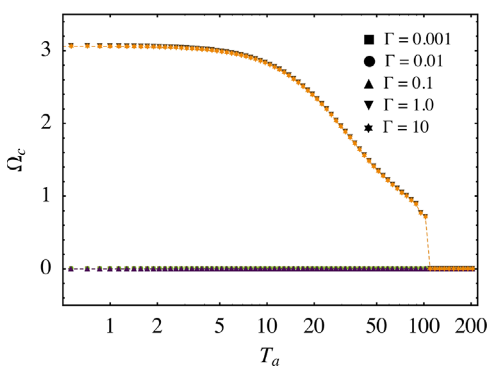


**Fig. 9.** $\Omega_c$ as a function of $T_a$ for different values of $\Gamma$ as in Fig. 8.

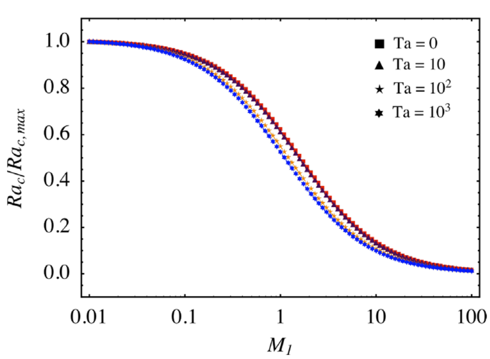


**Fig. 10.** $Ra_c/Ra_{c,\max}$ as a function of $M_1$ for different values of $T_a$ at $\Lambda = 0.5$, $\Gamma = 1$, $P = 10$ and $M_3 = 1.1$. The different values of $T_a$ are represented by different symbols from bottom to top $T_a = \{0, 10, 10^2, 10^3\} = \{■, ▴, ★, ✱\}$.

curve $Ra$ versus $k$. The minimum of this curve gives $Ra_c$ and $k_c$, and the corresponding value for the critical frequency $\Omega_c$.

Fig. 8 displays the critical Rayleigh number for different Deborah numbers, each normalized by its maximum value at $T_a = 100$, $Ra_c/Ra_{c,\max}$, as a function of the Taylor number. In all cases the relative threshold increases with the rotation rate. Viscoelastic effects have a different influence for small and intermediate values of $T_a$, but act similarly for larger values. The transitions can be stationary or oscillatory. To decide this the critical frequency, $\Omega_c$, has to be calculated. It is displayed as a function of $T_a$ in Fig. 9. For small Deborah numbers ($\Gamma \sim 10^{-4}$–$10^{-1}$) the critical frequency is zero and the convection is stationary irrespective of the rotation rate, while for intermediate and strong viscoelasticity ($\Gamma > 1$) the primary bifurcation is oscillatory for small values of $T_a$, but switches to stationary above a critical value of the Taylor number, $T_a \approx 109$.

Fig. 10 displays the normalized critical Rayleigh number, $Ra_c/Ra_{c,\max}$, as a function of the magnetic filed, $M_1 \propto H^2$, for different values of the Taylor number, $T_a$. In all cases the threshold decreases with increasing magnetic field as has also been found for free–free boundary conditions. Finally, let us comment that for small and intermediate values of $T_a$ the critical frequency increases with $M_1$, similar to the case without rotation [77], but for very large values, $T_a \sim 10^3$, the convection is always stationary.

## 4. Final remarks

In the present work, Rayleigh–Bénard rotating convection in a magnetic viscoelastic liquid is studied. The stability thresholds for both, the stationary and the oscillatory convection, have been determined. Two different boundary conditions for the velocity field were analyzed, the so-called free–free and rigid–rigid ones. For the former the results of Venkatasubramanian and Kaloni [29] for the stationary convection and of Perez and coworkers [77] for the oscillatory convection without rotation have been regained. In addition, we have provided analytical formula for the oscillatory convection in the small rotation as well as in the large Prandtl limit. For weakly viscoelastic fluids the critical Rayleigh number for the oscillatory convection is much higher than that for the stationary one, while for high Deborah numbers the oscillatory instability always precedes the stationary one. In this paper, we have also calculated the range of parameters, for which a codimension-2 bifurcation appears.

Due to the presence of various destabilizing effects, i.e., buoyancy and magnetic forces, and of additional relaxation channels due to the Oldroyd model, the discussion of the stability curves becomes rather intricate. An oscillatory instability, whose critical frequency is a rapidly varying function of the Deborah number, is competing with the stationary one. As a result, the codimension-2 bifurcation line, separating those two instabilities, strongly depends on the structure of the Oldroyd model and its relaxation times.

In the case of realistic rigid–rigid boundary conditions, the convection thresholds are calculated numerically by the spectral method. The technique of collocation points (Gauss-Lobato) as described in [84] was used. We have observed that the bifurcation scenario is changed compared to that for ideal free–free boundary conditions. In particular, we have found that in the realistic case, for large rotation rates, $T_a \gtrsim 10^2$, the primary bifurcation is stationary in a wide range of rheological parameters.

Finally, we want to mention that, very often, an external rotation induces other types of patterns, such as found in the Küppers–Lortz instability. To study such instabilities a nonlinear analysis is necessary. A detailed study of the weakly nonlinear analysis for rotating magnetic viscoelastic fluids is in progress.

## Acknowledgments

We thank H. Pleiner (MPI-P, Mainz) for useful discussions and his critical reading of the manuscript. The authors acknowledge partial financial support from FONDECYT 1120764, Millennium Scientific Initiative, P10-061-F, Basal Program Center for Development of Nanoscience and Nanotechnology (CEDENNA), UTA-project 8750-12, MICINN (Spanish Ministry of Science and Technology) under Project FIS2011-24642 and DIUFRO project under grant DI13-6000.

## Appendix A. Coefficients $\phi_i$

The coefficients $\{\phi_i\}$ of Eq. (43) are

$$\phi_0 = P^2q^2[q^8P\Gamma(1-\Lambda) - q^6(P+1) - q^2\pi^2\Gamma PT(1-\Lambda) + \pi^2T(1-P)], \tag{A.1}$$

$$\begin{aligned}\phi_2 = {} & q^{10}\Gamma^3P^3\Lambda^2(1-\Lambda) \\ & -3q^8\Gamma^2P^2(\Lambda^2+1) \\ & +q^8\Gamma^2P^2\Lambda(4-P(\Lambda+1)) \\ & +q^6\Gamma P(1-\Lambda)(2P+3) \\ & +q^4(P(\pi^2\Gamma^3P^2T(\Lambda-1)-1)-1) \\ & +q^2\pi^2(\Gamma^2P^2T(2-P(\Lambda+1))+2),\end{aligned} \tag{A.2}$$

$$\begin{aligned}\phi_4 = {} & \Gamma^2[q^8\Gamma^2\Lambda^2P^2(1-\Lambda P) \\ & -2q^6\Lambda^2P^2\Gamma^2 \\ & +q^6P\Gamma(1-\Lambda)(2\Lambda P+3) \\ & -q^4(P(\Gamma+1)+2) \\ & +q^2\pi^2P^2\Gamma^2T(1-\Lambda P)],\end{aligned} \tag{A.3}$$

$$\phi_6 = -q^4\Gamma^4(\Lambda P+1). \tag{A.4}$$

## References


[1] R.E. Rosensweig, Ferrohydrodynamics, Cambridge University Press, Cambridge, 1985.
[2] S. Odenbach, Ferrofluids: Magnetically Controllable Fluids and Their Applications, Springer, Berlin, 2003.
[3] S. Odenbach (Ed.), Colloidal Magnetic Fluids: Basics, Development and Application of Ferrofluids, Springer, Berlin, 2009.
[4] M. Mahmoudi, et al., J. Phys. Chem. C 113 (2009) 2322.
[5] E.H. Kim, Y. Ahn, H.S. Lee, J. Alloys Compds. 434 (2007) 633.
[6] C. Alexiou, et al., J. Drug Targeting 11 (2003) 139.
[7] C. Alexiou, et al., J. Magn. Magn. Mater. 252 (2002) 363.
[8] C. Alexiou, et al., Cancer Res. 60 (2000) 6641.
[9] A.S. Popel, P.C. Johnson, Annu. Rev. Fluid Mech. 37 (2005) 43.
[10] O.K. Baskurt, H.J. Meiselman, Sem. Throm. Hem. 29 (2003) 435.
[11] J.J. Bishop, Biorheology 38 (2001) 263.
[12] H. Shahnazian, et al., J. Phys. D: Appl. Phys. 42 (2009) 205004.
[13] D. Yu Borin, S. Odenbach, J. Phys.: Condens. Matter 21 (2009) 246002.
[14] S.A. Lira, J.A. Miranda, Phys. Rev. E 80 (2009) 046313.
[15] S.A. Lira, J.A. Miranda, Phys. Rev. E 79 (2009) 046303.
[16] O. Müller, D. Hahn, M. Liu, J. Phys.: Condens. Matter 18 (2006) S2623.
[17] P. Ilg, M. Kroger, S. Hess, Phys. Rev. E 71 (2005) 031205.
[18] S. Odenbach, J. Phys.: Condens. Matter 16 (2004) R1135.
[19] S. Odenbach, J. Phys.: Condens. Matter 15 (2003) S1497.
[20] H.W. Müller, M. Liu, Phys. Rev. E 64 (2001) 061405.
[21] B.J. de Gans, C. Blom, A.P. Philipse, J. Mellema, Phys. Rev. E 60 (1999) 4518.
[22] S. Odenbach, J. Magn. Magn. Mat. 201 (1999) 149.
[23] J.L. Neuringer, R.E. Rosensweig, Phys. Fluids 7 (1964) 1927.
[24] B.A. Finlayson, J. Fluid Mech. 40 (1970) 753.
[25] K. Gotoh, M. Yamada, J. Phys. Soc. Jpn. 51 (1982) 3042.
[26] P.J. Blennerhassett, F. Lin, P.J. Stiles, Proc. R. Soc. London A 433 (1991) 165.
[27] D. Laroze, P.G. Siddheshwar, H. Pleiner, Commun. Nonlinear Sci. Numer. Simulat. 18 (2013) 2436.
[28] M.D. Gupta, A.S. Gupta, Int. J. Eng. Sci. 17 (1979) 271.
[29] S. Venkatasubramanian, P.N. Kaloni, Int. J. Eng. Sci. 32 (1994) 237.
[30] P.N. Kaloni, J.X. Lou, J. Magn. Magn. Mater. 284 (2004) 54.
[31] G. K Auernhammer, H.R. Brand, Eur. Phys. J. B 16 (2000) 157.
[32] A. Ryskin, H. Pleiner, Phys. Rev. E 69 (2004) 046301.
[33] D. Laroze, J. Martinez-Mardones, J. Bragard, P. Vargas, Physica A 371 (2006) 46.
[34] D. Laroze, J. Martinez-Mardones, L.M. Pérez, Y. Rameshwar, Int. J. Bif. Chaos 19 (2009) 2755.
[35] Y. Qin, P.N. Kaloni, Eur. J. Mech. B/Fluids 13 (1994) 305.
[36] I.S. Shivakumara, N. Rudraiah, C.E. Nanjundappa, J. Magn. Magn. Mater. 248 (2002) 379.
[37] P.N. Kaloni, J.X. Lou, Phys. Rev. E 70 (2004) 026313.
[38] P.N. Kaloni, J.X. Lou, Phys. Rev. E 71 (2005) 066311.
[39] Sunil, P. Sharma, A. Mahajan, Heat. Trans. Res. 40 (2009) 351.
[40] Sunil, P. Chandb, P.K. Bhartia, A. Mahajan, J. Magn. Magn. Mater. 320 (2008) 316.
[41] S. Odenbach, Th. Volker, J. Magn. Magn. Mater. 289 (2005) 122.
[42] I.S. Shivakumara, Jinho Lee, C.E. Nanjundappa, M. Ravisha, Transp. Porous Med. 87 (2011) 251.
[43] A. Mahajan, M. Arora, Appl. Math. Comput. 219 (2013) 6284.
[44] A. Recktenwald, M. Lucke, J. Magn. Magn. Mater. 188 (1998) 326.
[45] Sunil, A. Mahajan, Proc. R. Soc. A 464 (2008) 83.
[46] Sunil, A. Mahajan, Appl. Math. Comp. 204 (2008) 299.
[47] I. Shliomis, B.L. Smorodin, J. Magn. Magn. Mater. 252 (2002) 197.
[48] R. Patel, Phys. Rev. E 85 (2012) 026316.
[49] K. Parekh, H.S. Lee, in: AIP Conference Proceedings, vol. 1447, 2012, p. 385.
[50] D.D. Joseph, Fluid Dynamics of Viscoelastic Liquids, Springer, New York, 1990.
[51] C.M. Vest, A. Arpaci, J. Fluid Mech. 36 (1969) 613.
[52] M. Sokolov, R.I. Tanner, Phys. Fluids 15 (1972) 534.
[53] T.P. Lyubimova, Izv. Akad. Nauk SSSR, Mekh. Zhidk. Gaza. 2 (1974) 181.
[54] K.J. Ropke, P. Schümmer, Rheol. Acta 21 (1982) 540.
[55] J. Stastna, J. Non-Newtonian Fluid Mech. 18 (1985) 61.
[56] S. Rosenblat, J. Non-Newtonian Fluid Mech. 21 (1986) 201.
[57] R.W. Kolkka, G.R. Ierly, J. Non-Newtonian Fluid Mech. 25 (1987) 299.
[58] N. Rudraiah, P.N. Kaloni, P.V. Radhadevi, Rheol. Acta 28 (1989) 48.
[59] J. Martinez-Mardones, C. Perez-Garcia, J. Phys. Condens. Matter 2 (1990) 1981.
[60] J. Martinez-Mardones, R. Tiemann, W. Zeller, C. Perez-Garcia, Int. J. Bif. Chaos 4 (1994) 1347.
[61] J. Martinez-Mardones, R. Tiemann, W. Zeller, Chaos Solit. Fract. 6 (1995) 341.
[62] J. Martinez-Mardones, R. Tiemann, D. Walgraef, W. Zeller, Phys. Rev. E 54 (1996) 1478.
[63] H.M. Park, H.S. Lee, J. Non-Newtonian Fluid Mech. 60 (1995) 1.
[64] H.M. Park, H.S. Lee, J. Non-Newtonian Fluid Mech. 66 (1996) 1.
[65] P. Parmentier, G. Lebon, V. Regnier, J. Non-Newtonian Fluid Mech. 89 (2000) 63.
[66] P. Parmentier, Etude thédorique des insdtabilités capillaires at gravifiques dans les fluides viscoélastiques (Ph.D. thesis), Université de Liège, 1997.
[67] P.N. Kaloni, J.X. Lou, J. Non-Newtonian Fluid Mech. 107 (2002) 97.
[68] P. Kolodner, J. Non-Newtonian Fluid Mech. 75 (1998) 167.
[69] J. Martinez-Mardones, R. Tiemann, D. Walgraef, J. Non-Newtonian Fluid Mech. 93 (2000) 1.
[70] J. Martinez-Mardones, R. Tiemann, D. Walgraef, Physica A 327 (2003) 29.
[71] D. Laroze, J. Martinez-Mardones, C. Perez-Garcia, Int. J. Bif. Chaos 15 (2005) 3329.
[72] D. Laroze, J. Martinez-Mardones, J. Bragard, C. Perez-Garcia, Physica A 385 (2007) 433.
[73] D. Laroze, J. Martinez-Mardones, J. Bragard, Eur. Phys. J. Spec. Top. 146 (2007) 291.
[74] D. Laroze, J. Martinez-Mardones, L.M. Pérez, Int. J. Bif. Chaos 20 (2010) 235.
[75] D. Laroze, J. Martinez-Mardones, L.M. Pérez, R.G. Rojas, J. Magn. Magn. Mat. 322 (2010) 3576.
[76] D. Laroze, L.M. Pérez, J. Bragard, E.G. Cordaro, J. Martinez-Mardones, Magnetohydrodynamics 47 (2011) 159.
[77] L.M. Pérez, J. Bragard, D. Laroze, J. Martinez-Mardones, H. Pleiner, J. Magn. Magn. Mater. 323 (2011) 691.
[78] D. Laroze, J. Martinez-Mardones, H. Pleiner, Eur. Phys. J. Spec. Top. 219 (2013) 71.
[79] T.T. Perkins, D.E. Smith, S. Chu, Science 276 (1997) 2016.
[80] S.R. Quake, H. Babcock, S. Chu, Nature 388 (1997) 151.
[81] H. Babcock, D.E. Smith, J.S. Hur, E.S.G. Shaqfeh, S. Chu, Phys. Rev. Lett. 85 (2000) 2018.
[82] S. Chandrasekhar, Hydrodynamic and Hydromagnetic Stability, Dover, New-York, 1981.
[83] H. Pleiner, M. Liu, H.R. Brand, Rheol. Acta 43 (2004) 502.
[84] L.N. Trefethen, Spectral Methods in Matlab, SIAM, Philadelphia, 2000.